

Arterial Luminal Curvature and Fibrous-Cap Thickness Affect Critical Stress Conditions Within Atherosclerotic Plaque: An *In Vivo* MRI-Based 2D Finite-Element Study

ZHONGZHAO TENG,¹ UMAR SADAT,¹ ZHIYONG LI,^{1,2} XUEYING HUANG,³ CHENGCHENG ZHU,¹
VICTORIA E. YOUNG,¹ MARTIN J. GRAVES,¹ and JONATHAN H. GILLARD¹

¹University Department of Radiology, University of Cambridge, Cambridge, UK; ²School of Biological Science & Medical Engineering, Southeast University, Nanjing, China; and ³Department of Mathematics, Xiamen University, Xiamen, China

(Received 26 January 2010; accepted 13 May 2010; published online 25 May 2010)

Associate Editor Jane Grande-Allen oversaw the review of this article.

Abstract—High mechanical stress in atherosclerotic plaques at vulnerable sites, called critical stress, contributes to plaque rupture. The site of minimum fibrous cap (FC) thickness (FC_{MIN}) and plaque shoulder are well-documented vulnerable sites. The inherent weakness of the FC material at the thinnest point increases the stress, making it vulnerable, and it is the big curvature of the lumen contour over FC which may result in increased plaque stress. We aimed to assess critical stresses at FC_{MIN} and the maximum lumen curvature over FC (LC_{MAX}) and quantify the difference to see which vulnerable site had the highest critical stress and was, therefore, at highest risk of rupture. One hundred patients underwent high resolution carotid magnetic resonance (MR) imaging. We used 352 MR slices with delineated atherosclerotic components for the simulation study. Stresses at all the integral nodes along the lumen surface were calculated using the finite-element method. FC_{MIN} and LC_{MAX} were identified, and critical stresses at these sites were assessed and compared. Critical stress at FC_{MIN} was significantly lower than that at LC_{MAX} (median: 121.55 kPa; inter quartile range (IQR) = [60.70–180.32] kPa vs. 150.80 kPa; IQR = [91.39–235.75] kPa, $p < 0.0001$). If critical stress at FC_{MIN} was only used, then the stress condition of 238 of 352 MR slices would be underestimated, while if the critical stress at LC_{MAX} only was used, then 112 out of 352 would be underestimated. Stress analysis at FC_{MIN} and LC_{MAX} should be used for a refined mechanical risk assessment of atherosclerotic plaques, since material failure at either site may result in rupture.

Keywords—Curvature, Atherosclerosis, Stress, Plaque rupture, MRI.

INTRODUCTION

Atherosclerotic plaques may rupture without warning and cause acute thromboembolic events, such as myocardial infarction and ischemic strokes. Angiography usually identifies atheromatous lesions that encroach significantly into the lumen. There is a poor correlation between the angiographic appearance and subsequent risk of clinic event in carotid artery¹⁶ with more than 80% of ischemic events occurring in lesions that cause less than 70% stenosis in coronary arteries.⁷ There is, therefore, a need of a diagnostic technique that reflects plaque morphology, underlying inflammatory activity and structural stability rather than luminal stenosis alone. Magnetic resonance imaging (MRI) is able to quantify carotid plaque composition with good accuracy and reproducibility.⁴ Plaque morphology studies indicate that a large atheromatous lipid-rich core, a thin fibrous cap (FC) with or without erosions/disruptions and the presence of plaque haemorrhage have a strong association with plaque rupture.^{2,3,5,14,18,26} Results of MRI- and histology-based finite element method studies reveal higher mechanical stresses at the rupture site.^{12,15,20} The mechanical assessment of plaques should therefore be considered in an integrated way with their morphology for a refined plaque vulnerability assessment.

Plaque rupture usually occurs at the site of minimum FC thickness (FC_{MIN}) or at the plaque shoulder where the curvature is locally large (i.e. acute angulation is present). FC_{MIN} becomes a vulnerable site as it becomes thin from underlying inflammation. Plaque shoulders also show features of high underlying inflammation^{15,19} making them vulnerable. From a biomechanical point view, it is the acute angulation of

Address correspondence to Dr. Zhongzhao Teng, University Department of Radiology, University of Cambridge, Level 5, Box 218, Addenbrooke's Hospital, Hills Road, Cambridge CB2 0QQ, UK. Electronic mail: zt215@cam.ac.uk

the lumen contour that may enhance the plaque stresses at that site. We decided to assess the mechanical stresses at FC_{MIN} and at the site of maximum lumen curvature over the diseased region (LC_{MAX}) i.e. maximum acute angulation. This was done to see whether there was any significant difference between the stresses at these vulnerable sites (i.e. “critical stresses”) and whether either of them alone was reliable enough to provide information about critical plaque stresses and, therefore, act as a risk assessment tool. This is because the extra loading exceeding the material strength of FC at either site will possibly lead to plaque rupture.

MATERIALS AND METHODS

MRI Acquisition

One hundred (100) patients (Age: 70.8 ± 11.2 ; 77 males) with atherosclerotic carotid artery disease underwent high-resolution black-blood MRI of their symptomatic carotid artery. Axial T_1 , T_2 , and short tau inversion recovery (STIR) weighted images covering the entire carotid plaque were acquired (Fig. 1a) using these MR parameters: T_1 weighted (repetition time/echo time: $1 * RR/7.8$ ms) with fat saturation; T_2 weighted (repetition time/echo time: $2 * RR/100$ ms) with fat saturation; and STIR (repetition time/echo time/inversion time: $2 * RR/46$ ms/150 ms).²⁵ The field of view was 10×10 cm and matrix size 256×256 . The in plane spatial resolution achieved was of the order of 0.39×0.39 mm 2 . Manual segmentation of plaque components was performed using previously published criteria, to identify FC, lipid pool (Lip), calcification (Ca), and plaque haemorrhage (PH)²³ (Fig. 1b). All the segmented contours were interpolated with 200–400 equidistant points using cubic spline function to avoid segmentation distortion. In total, 352 slices with atherosclerotic components were used for the computational study.

Curvature and Thickness of Fibrous Cap

As shown in Fig. 1c, the local curvature at point a was computed using the radius of the circle, determined by point a and the adjacent points (white dots in the figure) on both sides. The distance was measured between point a and the intersection (b) of the component contour and the line connecting the center of the circle and a . Local curvature depends on the spacing of the points along the boundary. However, when the distance between two points is small enough, the curvature is point number independent. In this study, when the point number is larger than 200,

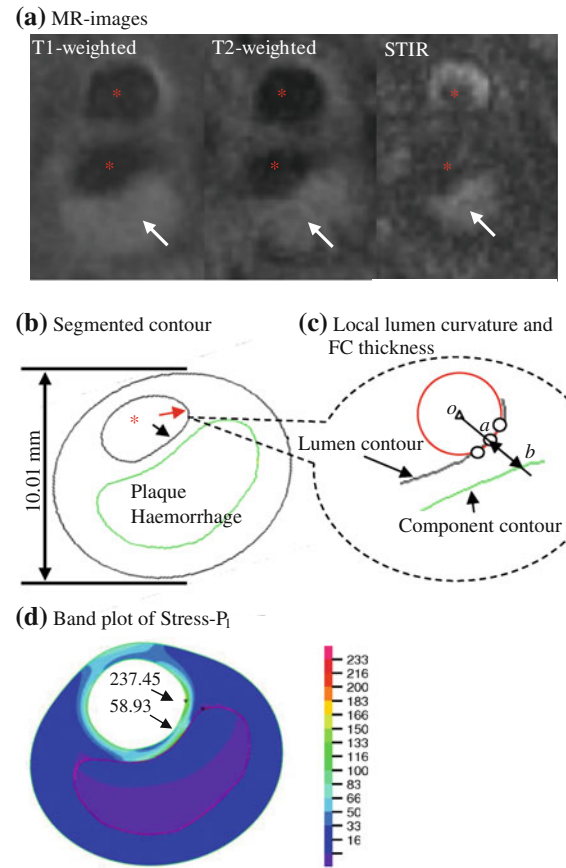


FIGURE 1. (a) Multi-sequence high resolution *in vivo* MR-image showing plaque components (haemorrhage marked by white arrow), lumen (marked by red asterisk) and wall boundaries; (b) Segmented plaque contour (red arrow points to local maximum fibrous cap (FC) curvature, and black arrow points to the location with local minimum FC thickness); (c) Schematic drawing showing the definitions of local FC thickness and curvature; (d) Band plot of Stress- P_1 (unit: kPa) distribution at systole. Stress- P_1 is very different at locations with local maximum FC curvature (LC_{MAX}) and minimum FC thickness (FC_{MIN}).

the difference in computing the curvature is not observable.

Finite Element Simulation

As the *in vivo* MR-images were obtained at the diastolic cardiac point, a pre-shrink process is necessary to obtain the zero pressurized shape which has been discussed in detail previously.^{6,9,17,20,21} In this study, for each patient, the shrinkage was determined by choosing the most round slice which would recover its *in vivo* shape best when diastolic pressure was imposed. The shrinkage rates of lumen contour and outer wall were numerically determined following an iterative procedure so that: (1) the vessel cross-sectional

area was conserved (conservation of mass); and (2) the pressurized morphology and the original *in vivo* morphology had the best match. The determined lumen shrinkage was applied to all the slices of this patient. The lumen shrinkage rate was $9.61 \pm 2.04\%$ for the 100 patients in this study.

The plaque components were assumed to be hyperelastic as described by modified Mooney-Rivlin strain energy density function,

$$W = c_1(I_1 - 3) + D_1 \exp[D_2(I_1 - 3) - 1], \quad I_1 = \Sigma C_{ii}$$

where I_1 is the first strain invariants, $\mathbf{C} = \mathbf{F}^T \mathbf{F}$ is the right Cauchy-Green deformation tensor, $\mathbf{F} = [F_{ij}] = [\partial x_i / \partial \alpha_j]$, $[x_i]$ is current position, $[\alpha_i]$ is original position, c_1 , D_1 , and D_2 are material parameters which are adopted from earlier studies.^{1,20} The blood pressure for each patient, measured before MRI, was used as the loading condition to perform the patient-specific simulation. Maximum principle stress (Stress-P₁) was generated using finite element method and solved in ADINA8.6 (ADINA, Inc.) (Fig. 1d). A finer mesh was used for slices with larger lumen curvature or thin FC by increasing the interpolation point number.

Definition and Calculation of Critical Stress

The maximum value of Stress-P₁ at all vulnerable sites with local minimum FC thickness of each slice was used as the thickness-related critical stress (T-CStress) of that MR slice. The maximum value of Stress-P₁ at all locations with local largest lumen curvature was adopted as the curvature-related critical stress (C-CStress) for that slice. In order to be assessed for lumen curvature analysis, the curvature sites had to overlie an underlying plaque component. Healthy sites, where no plaque component was present and rupture was unlikely, were excluded from the analysis.

Statistical Analysis

The normality of data was assessed using Shapiro-Wilk test. Mann-Whitney test was used for the statistical analysis. A significant difference was considered only if $p < 0.05$. GraphPad InStat 3.06 was used for analysis.

RESULTS

As shown in Fig. 1b, the locations of local large curvature (marked by red arrow) and minimum local FC thickness (marked by black arrow) are not identical, and Stress-P₁ at each location (Fig. 1d) is different. For all the 352 slices, the median value of T-CStress was 121.55 kPa (Inter Quartile Range, IQR = [69.70,

180.32] kPa). It was significantly lower than C-CStress (150.80 kPa, IQR = [91.39, 235.75] kPa), ($p < 0.0001$). The visualized comparison is shown in Fig. 2. It implies that adopting the stress from FC_{MIN} will underestimate the critical condition by approximately 20%. Compared with the thickness concept, the local maximum curvature concept will give a better plaque risk assessment.

Further analysis indicated that critical stress from location with either minimum FC thickness or the largest lumen curvature alone cannot provide accurate mechanics-based plaque risk assessment. Because these two geometric features are often located at different locations and the corresponding stress levels are very different (Fig. 3). Of the 352 slices, 67.6% (238 slices) will be underestimated using the thickness concept; however, 31.8% (112 slices) will be underestimated using the curvature concept only. Only two slices had identical locations of FC_{MIN} and LC_{MAX}. In mechanical terms, failure at either site will lead to the plaque rupture and cause a fatal event. Thus, the maximum of the T-CStress and C-CStress (M-CStress) may be a better indicator than either T-CStress or C-CStress alone for stress-based plaque vulnerability

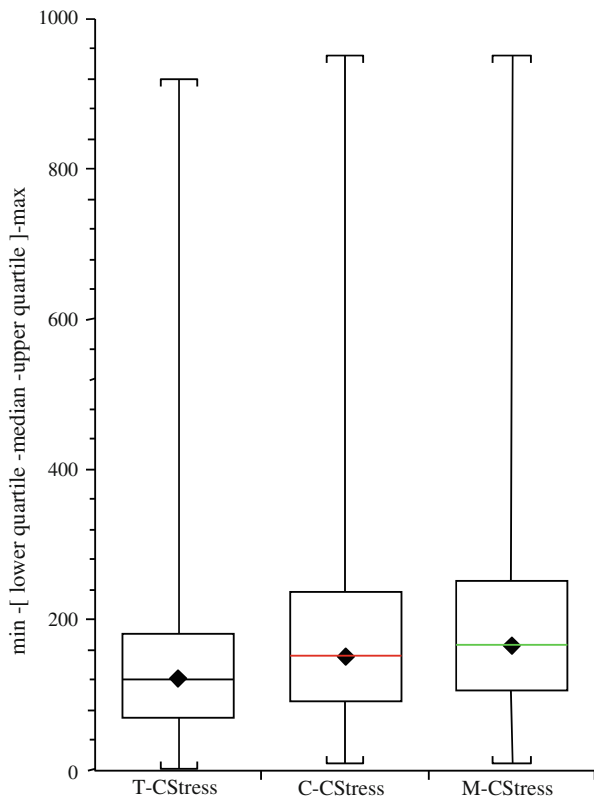


FIGURE 2. Comparisons among Stress-P₁ from the locations with local minimum FC thickness (T-CStress), local maximum FC curvature (C-CStress) and their maximum value (M-CStress).

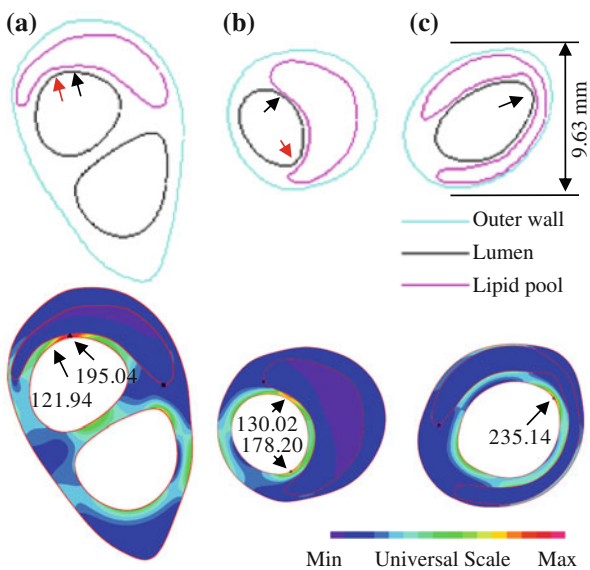


FIGURE 3. Critical stresses at different vulnerable sites (Unit: kPa). (a) T-CStress is higher than C-CStress; (b) T-CStress is lower than C-CStress; (c) T-CStress and C-CStress are located at an identical vulnerable site.

assessment. As shown in Fig. 2, M-CStress (median: 165.54 kPa, IQR = [105.76, 252.24] kPa) is significantly higher than T-CStress ($p < 0.0001$). Although no significant difference is found between M-CStress and C-CStress ($p = 0.0721$), the median value is about 10% higher when M-CStress is adopted for risk assessment.

DISCUSSION

A detailed analysis of the plaque vulnerable sites and the mechanical conditions therein is essential for a better understanding of the pathomechanics of plaque rupture. Numerous efforts have been made in this regard. By using 3D fluid–structure interaction models, Tang *et al.*²⁰ showed that the rupture location in the carotid plaque was at the site of minimum FC thickness. A ‘local maximal stress hypothesis’ was introduced to identify the vulnerable site for both coronary²² and carotid²¹ plaque, and the stress condition at the minimum FC thickness site was proposed to be an indicator for plaque vulnerability assessment. Richardson *et al.*¹⁵ found that in the 67 patients with eccentric lipid pool, who had died from coronary thrombosis, 63% of coronary plaques fissured in the shoulder area, and both stress and foam cell concentrations were found at the tear site. Li *et al.*¹³ used idealized geometric models to represent that stress contraction appeared at the site with large lumen curvature, and further analysis indicated that lumen curvature of the carotid plaque of symptomatic patients was much larger than that of asymptomatic patients.

Tang *et al.*¹⁹ discovered that the high stress at the thin FC and the shoulder area was associated with plaque inflammation in the carotid plaque using USPIO-enhanced (ultra small super-paramagnetic iron oxide) MRI. However, high mechanical stress linking to plaque rupture still remains a hypothesis. A large scale follow-up study is needed to validate this hypothesis.

This is the first study to our knowledge in which the efficacy of lumen curvature for the biomechanical stress analysis of plaque vulnerable site assessment has been demonstrated and the difference between the mechanical conditions at different vulnerable sites has been investigated. As atherosoma enlarges, it may protrude into the lumen resulting in an irregular lumen shape with varying lumen curvature. The most common site of the acute angulation of lumen curvature is the plaque shoulder area which is considered as a vulnerable site for plaque rupture. Histological analysis has revealed a high concentration of macrophages and mast cells in this area.¹⁵ The release of various proteolytic agents by these inflammatory cells weakens the plaque structure thereby significantly reducing the material strength.^{10,11} Although the shoulder region has a relatively thick FC thickness, there is high biomechanical stress which most likely results from the increased lumen curvature (acute angulation) making it a vulnerable site. The other well-documented vulnerable site is the location of minimum FC thickness. It is, however, a naturally vulnerable site because of the inherent weakness of thin FC resulting from the high underlying inflammation. Failure at either of minimum FC thickness or large curvature, therefore, may lead to plaque rupture. It is therefore logical to evaluate these vulnerable sites by using biomechanical simulations. Although high stresses are present at both FC_{MIN} and LC_{MAX} , by using one of them alone, critical stress levels would have been underestimated as observed in this study. Maximum Stress- P_1 at FC_{MIN} and LC_{MAX} may, therefore, be a better indicator for plaque vulnerability assessment.

We were also successful in assessing the effect of plaque components on stress distribution; computing the mechanical force involves information about plaque morphology and material properties of its components. Although each of these significantly governs the stress distribution nonlinearly, we were able to quantify some important features: the critical stress is usually found in the region covering soft components such as lipid core and haemorrhage. In this study, M-CStress was identified at the region covering lipid core or haemorrhage in 69.3% (244 out of 352) of slices. M-CStress appeared at the region of fibrous tissue in only 29.3% of slices ($n = 103$) and only 1.4% of slices ($n = 5$), M-CStress was located in the region covering hard component, such as calcification.

This study has a few limitations such as (1) histological analysis of atheromas was not done for correlation with MR images. However, this validation has already been done by our group.^{23,24} (2) The FC thickness measurement was critical in this study. However, due to MR spatial resolution being limited to 0.39 mm, there is a possibility that thinner FCs below this resolution have been underestimated. With possible improvement in MRI techniques in future, this limitation may be overcome. (3) The lumen shrinkage of each plaque was determined using a relatively round artery contour. It might not be true for slices with heavy plaque burden, and, therefore, for a refined simulation, slice-specific shrinkage should be determined. (4) Because this was not a 3D fluid structure interaction model, it was not possible to simulate the effect of turbulent flow and a pressure drop across a stenosis, which of course will affect the applied load. (5) Moreover, the residual stress was not considered since it is not measurable with current MR technique,⁸ and the plaque was treated as a piecewise homogenous material and the patient-specific material properties were not considered.

ACKNOWLEDGMENTS

This research is partly supported by ARTreat FP7 Europain Union and NIHR Cambridge Biomedical Research Centre. Dr. Umar Sadat is funded by the Medical Research Council & Royal College of Surgeons of England Joint Clinical Research Training Fellowship. We thank Tim Baynes from University of Cambridge for proof reading of this manuscript.

REFERENCES

- ¹Aglyamov, S. R., A. R. Skovoroda, H. Xie, K. Kim, J. M. Rubin, M. O'Donnell, T. W. Wakefield, D. Myers, and S. Y. Emelianov. Model-based reconstructive elasticity imaging using ultrasound. *Int. J. Biomed. Imaging* 2007:11, 2007.
- ²Bock, R. W., A. C. Gray-Weale, P. A. Mock, *et al.* The natural history of asymptomatic carotid artery disease. *J. Vasc. Surg.* 17:160–169, 1993 (discussion 170–171).
- ³Boyle, J. J. Association of coronary plaque rupture and atherosclerotic inflammation. *J. Pathol.* 181:93–99, 1997.
- ⁴Cai, J. M., T. S. Hatsuhami, M. S. Ferguson, *et al.* Classification of human carotid atherosclerotic lesions with in vivo multicontrast magnetic resonance imaging. *Circulation* 106:1368–1373, 2002.
- ⁵Corti, R., R. Hutter, J. J. Badimon, and V. Fuster. Evolving concepts in the triad of atherosclerosis, inflammation and thrombosis. *J. Thromb. Thrombolysis*. 17:35–44, 2004.
- ⁶de Putter, S., B. J. Wolters, M. C. Rutten, *et al.* Patient-specific initial wall stress in abdominal aortic aneurysms with a backward incremental method. *J. Biomech.* 40:1081–1090, 2007.
- ⁷Falk, E., P. K. Shah, and V. Fuster. Coronary plaque disruption. *Circulation* 92:657–671, 1995.
- ⁸Fung, Y. C. What are the residual stresses doing in our blood vessels? *Ann. Biomed. Eng.* 19:237–249, 1991.
- ⁹Huang, X., C. Yang, C. Yuan, *et al.* Patient-specific artery shrinkage and 3D zero-stress state in multi-component 3D FSI models for carotid atherosclerotic plaques based on in vivo MRI data. *Mol. Cell. Biomech.* 6:121–134, 2009.
- ¹⁰London, C. L., M. J. Davies, G. V. Born, and P. D. Richardson. Atherosclerotic plaque caps are locally weakened when macrophages density is increased. *Atherosclerosis* 87:87–90, 1991.
- ¹¹London, C. L., M. J. Davies, P. D. Richardson, and G. V. Born. Testing of small connective tissue specimens for the determination of the mechanical behaviour of atherosclerotic plaques. *J. Biomed. Eng.* 15:27–33, 1993.
- ¹²Li, Z. Y., S. Howarth, R. A. Trivedi, *et al.* Stress analysis of carotid plaque rupture based on in vivo high resolution MRI. *J. Biomech.* 39:2611–2622, 2006.
- ¹³Li, Z. Y., T. Tang, J. U-King-Im, M. Graves, M. Sutcliffe, and J. H. Gillard. Assessment of carotid plaque vulnerability using structural and geometrical determinants. *Circ. J.* 72:1092–1099, 2008.
- ¹⁴Redgrave, J. N., P. Gallagher, J. K. Lovett, and P. M. Rothwell. Critical cap thickness and rupture in symptomatic carotid plaques: the oxford plaque study. *Stroke* 39:1722–1729, 2008.
- ¹⁵Richardson, P. D., M. J. Davies, and G. V. Born. Influence of plaque configuration and stress distribution on fissuring of coronary atherosclerotic plaques. *Lancet* 2:941–944, 1989.
- ¹⁶Rothwell, P. M., M. Eliasziw, S. A. Gutnikov, *et al.* Analysis of pooled data from the randomised controlled trials of endarterectomy for symptomatic carotid stenosis. *Lancet* 361:107–116, 2003.
- ¹⁷Speelman, L., E. M. Bosboom, G. W. Schurink, *et al.* Initial stress and nonlinear material behavior in patient-specific AAA wall stress analysis. *J. Biomech.* 42:1713–1719, 2009.
- ¹⁸Takaya, N., C. Yuan, B. Chu, *et al.* Association between carotid plaque characteristics and subsequent ischemic cerebrovascular events: a prospective assessment with MRI—initial results. *Stroke* 37:818–823, 2006.
- ¹⁹Tang, T. Y., S. P. Howarth, Z. Y. Li, *et al.* Correlation of carotid atheromatous plaque inflammation with biomechanical stress: utility of USPIO enhanced MR imaging and finite element analysis. *Atherosclerosis* 196:879–887, 2008.
- ²⁰Tang, D., Z. Teng, G. Canton, *et al.* Sites of rupture in human atherosclerotic carotid plaques are associated with high structural stresses: an in vivo MRI-based 3D fluid–structure interaction study. *Stroke* 40:3258–3263, 2009.
- ²¹Tang, D., Z. Teng, G. Canton, *et al.* Local critical stress correlates better than global maximum stress with plaque morphological features linked to atherosclerotic plaque vulnerability: an in vivo multi-patient study. *Biomed. Eng. Online* 8:15, 2009.
- ²²Tang, D., C. Yang, J. Zheng, *et al.* Local maximal stress hypothesis and computational plaque vulnerability index for atherosclerotic plaque assessment. *Ann. Biomed. Eng.* 33:1789–1801, 2005.

- ²³Trivedi, R. A., J. M. U-King-Im, M. J. Graves, *et al.* MRI-derived measurements of fibrous-cap and lipid-core thickness: the potential for identifying vulnerable carotid plaques in vivo. *Neuroradiology* 46:738–743, 2004.
- ²⁴Trivedi, R. A., J. M. U-King-Im, M. J. Graves, *et al.* Multi-sequence in vivo MRI can quantify fibrous cap and lipid core components in human carotid atherosclerotic plaques. *Eur. J. Vasc. Endovasc. Surg.* 28:207–213, 2004.
- ²⁵U-King-Im, J. M., T. Y. Tang, A. Patterson, *et al.* Characterisation of carotid atheroma in symptomatic and asymptomatic patients using high resolution MRI. *J. Neurol. Neurosurg. Psychiatry* 79:905–912, 2008.
- ²⁶van der Wal, A. C., A. E. Becker, C. M. van der Loos, and P. K. Das. Site of intimal rupture or erosion of thrombosed coronary atherosclerotic plaques is characterized by an inflammatory process irrespective of the dominant plaque morphology. *Circulation* 89:36–44, 1994.